Effects of the Fermi-surface shrinking on the optical sum rule in pnictides

L. Benfatto and E. Cappelluti

Institute for Complex Systems (ISC), CNR, U.O.S. Sapienza and Department of Physics, Sapienza University of Rome, P. le A. Moro 2, 00185 Rome, Italy

(Received 29 November 2010; revised manuscript received 14 January 2011; published 22 March 2011)

In this paper, we investigate the effects of the band shifts induced by the interband spin-fluctuation coupling on the optical sum rule in pnictides. We show that, despite the shrinking of the Fermi surfaces with respect to first-principles calculations, the charge-carrier concentration in each band is almost unchanged, with a substantial conservation of the total optical sum rule. However, a significant transfer of spectral weight occurs from low-energy coherent processes to incoherent ones that is carried out integrating the data up to a finite cutoff, with practical consequences on the experimental estimate of the sum rule. This has profound consequences both on the absolute value of the sum rule and on its temperature dependence, which must be taken into account while discussing optical experiments in these systems.

DOI: 10.1103/PhysRevB.83.104516 PACS number(s): 74.20.−z, 74.70.Xa, 74.25.nd, 74.25.Jb

I. INTRODUCTION

Since the discovery of superconductivity in iron-based superconductors, a renewed interest has emerged in the properties of interacting multiband systems. Indeed, all the families of pnictides are semimetals, with several small hole and electron pockets at the Fermi level, originating from almost empty hole and electron bands. Such a topology has been predicted by density-functional-theory (DFT) calculations and confirmed by several experiments sensitive to the Fermi surface structure, such as de Haas–van Alphen[1–3] and angle-resolved photoemission spectroscopy (ARPES).[4–7] Despite the qualitative agreement with DFT predictions as far as the number and the character of the bands is concerned, the experimental data suggest the existence in the real materials of a band narrowing operating over an energy scale of hundredths of meV and of a shrinking of the Fermi surface areas with respect to DFT.

The first feature has been associated with the presence of electronic correlations[8,9] leading to an enhancement of the band mass m of the carriers with respect to the DFT value $m_{\rm DFT}$, in agreement with several DFT + Dynamical Mean Field Theory (DMFT) calculations giving $m \simeq 2m_{\rm DFT}$. This effect can possibly be detected also by an experimental estimate of the optical sum rule, which relates the integrated optical conductivity $\sigma(\omega)$ to the carrier density n and band mass, $W = \int_0^\infty d\omega\sigma(\omega) \propto n/m$.[10,11] Indeed, recent experiments in LaFePO show that the experimental weight $W_{\rm exp}$ is significantly reduced with respect to the DFT value, $W_{\rm exp}/W_{\rm DFT} \approx 0.5$.[12] Assuming that DFT correctly estimates the number of carriers n in each band, this result can be interpreted thus as an effect of the band-mass renormalization mentioned above, $W_{\rm exp}/W_{\rm DFT} \sim m_{\rm DFT}/m$.

In addition to the electronic correlations operating on large energy scales, a retarded low-energy interaction, mediated by the spin fluctuations, is also present in pnictides.[13,14] Within this context, the shrinking of the Fermi surface areas has been explained as an effect of the band shifts originating from the interband coupling of electron and hole bands mediated by low-energy spin fluctuations.[15] It is worth noting that these Fermi-surface shrinkings do not violate the total charge conservation, which, in multiband systems, is determined by the balance of the charge carriers in *all* the bands. In contrast to the many-body picture, an alternative explanation for the Fermi-surface shrinkings has been proposed to be an intrinsic inaccuracy of the DFT calculations in determining the energy of the band edges with respect to the Fermi level.[16] In this case, a simple rigid shift of the DFT bands could account for the observed shrinking of the Fermi surface areas[1] without involving many-body interaction effects. A natural consequence of this shift would be a reduction of the carrier concentration in real materials with respect to the DFT prediction, with direct implications for the optical sum rule. Indeed, the experimental observation of a low value of $W_{\rm exp}$ could not be attributed only to mass-renormalization effects, but should be associated (at least in part) with a reduction of n due to the rigid-band shift.[16,17]

Motivated by this framework, in this paper we present an extensive analysis of the effect of the Fermi-surface shrinking induced by the interband interactions on the charge-carrier conservation and on the optical properties of a multiband system. In particular, we show that within this context, in contrast to a Fermi-surface shrinking induced by a rigid-band shift,[16] the charge-carrier concentration in each band does *not* scale with the Fermi area, and it is instead only weakly affected by its shrinking, leading to a redistribution of spectral weight between coherent and incoherent processes and to a substantial conservation of the optical sum rule with respect to the noninteracting case. Notably, as we will show, the redistribution of optical spectral weight is remarkably different with respect to the rigid-band shift suggested in Ref. 16, where the reduction of the Fermi area is reflected in a corresponding reduction of *both* the Drude peak and the incoherent band (Fig. 1). On the contrary, in the case of a Fermi-surface shrinking induced by the retarded interband interactions, the reduction of the coherent Drude part associated with the Fermi-surface shrinking is accompanied by an additional transfer of spectral weight to incoherent processes [Fig. 1(c)]. As we shall see, this has practical consequences on the experimental determination of the optical sum rule, which is usually carried out integrating the data up to a finite cutoff.

The structure of the paper is the following. In Sec. II, we introduce the model and we show how in a multiband system with interband interactions the charge-carrier concentration

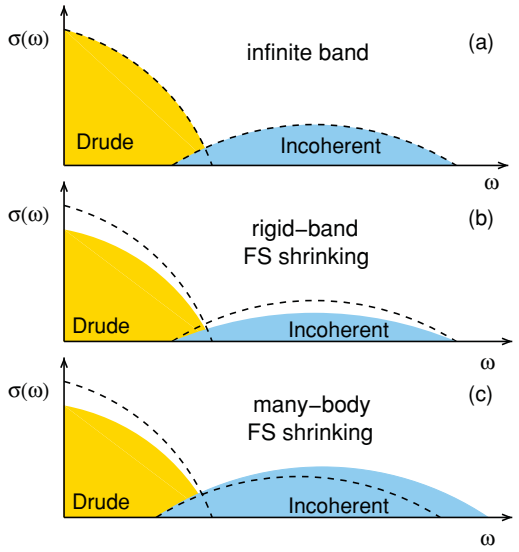

FIG. 1. (Color online) Sketch of the optical conductivity in three representative cases: (a) Infinite-band system interacting with a bosonic mode. The optical conductivity is characterized by a coherent Drude peak and an incoherent band. No Fermi-surface shrinking is present. (b) Same as in (a), but with a Fermi-surface shrinking due to a rigid-band shift. In this case, both the Drude peak and the weight of the incoherent processes are reduced. (c) Effects of a Fermi-surface shrinking due to a many-body interaction in a multiband system. In this case, the total spectral weight is (almost) unchanged, but the Fermi-surface shrinking reflects in a reduction of the coherent spectral weight in the Drude part, with an additional increase of the incoherent processes.

in each band does not scale with the corresponding Fermi-surface area. In Sec. III, we compute the optical conductivity in the presence of interactions and we analyze the effects of the Fermi-surface shrinking on the optical spectra. In Sec. IV, we focus on the temperature effects on the optical-conductivity sum rule by considering a bosonic spectrum that is either constant in temperature or temperature-dependent. In Sec. V, we comment on the outcomes of our results for the experiments in pnictides. In Sec. VI, we summarize our conclusions.

II. FERMI-SURFACE SHRINKING AND NUMBER OF CARRIERS

In this paper, we investigate the effect of a retarded interaction on the optical properties of a multiband system characterized by two peculiar features: (i) a strong particle-hole asymmetry of the bands and (ii) a predominant interband character of the interaction. The outcomes of these features on the one-particle properties have been discussed in Refs. 15 and 18, and the main results relevant to the present analysis will be recalled below. We will then follow here the same effective low-energy multiband scheme of Refs. 15 and 18, which contains also the main ingredients needed to discuss the physics of iron-based superconductors. In particular, we will focus on the parameter values appropriate for LaFePO, where both de Haas–van Alphen measurements of the Fermi-surface shrinking[1] and measurements of the optical conductivity[12] are available in the literature.

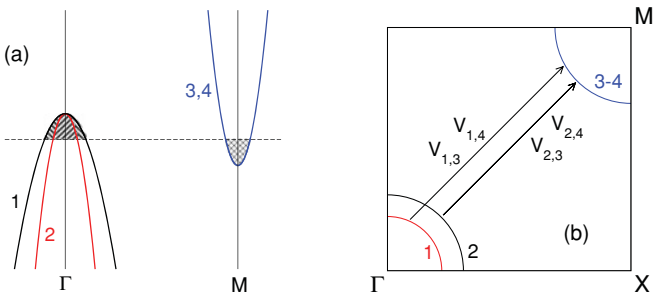

FIG. 2. (Color online) Sketch of the band structure and of the Fermi surfaces with the main interband interactions.

We consider two holelike bands (1,2) located close to the Γ point and two electronlike degenerate bands (3,4) close to the M point (see Fig. 2). All the bands close to the Fermi level can be schematized as parabolic,

$$\epsilon_{\mathbf{k},\alpha} = E_{\max,\alpha} - \frac{\hbar^2|\mathbf{k}|^2}{2m_\alpha}, \quad \alpha = 1,2 \tag{1}$$

for the hole bands and

$$\epsilon_{\mathbf{k},\alpha} = E_{\min,\alpha} + \frac{\hbar^2|\mathbf{k}|^2}{2m_\alpha}, \quad \alpha = 3,4, \tag{2}$$

for the electron ones, respectively. We assume also that carriers interact via a bosonic mode with a typical energy scale ω_0. In the case of pnictides, where the largest source of interactions comes from the exchange of spin fluctuations between quasinested hole and electron pockets, the interactions $V_{\alpha\beta}$ between two bands α and β will have a predominant interband character. As has been discussed in Ref. 18, the coupling to a low-energy mode cannot account for the overall reduction of the bandwidth with respect to DFT observed in ARPES experiments. This effect must be attributed to Coulomb repulsion occurring at high-energy scales,[8,9] and we model it by assuming our input masses as a factor of two larger than the DFT estimate, $m_\alpha \approx 2m_{\alpha,\mathrm{DFT}}$.[15,18] To be more explicit, setting for convention the Fermi level $\mu = 0$, we first estimate from DFT calculations the Fermi vectors $k_{F,\alpha}$ and the nearest band edge for each band, namely $E_{\max,1}$,$E_{\max,2}$ for the holelike bands and $E_{\min,3}$,$E_{\min,4}$ for the electronlike ones. From these we estimate the noninteracting mass for each band, $m_\alpha = \hbar^2 k_{F,\alpha}^2/2E_{\max(\min),\alpha}$, and the corresponding bare density of states $N_\alpha^0 = m_\alpha a^2/2\pi\hbar^2$ (where a is the in-plane lattice constant). Accordingly, the effective band edge far from the Fermi level[19] follows from the relation $N_\alpha^0 = 1/(E_{\max,\alpha} - E_{\min,\alpha})$. Finally, to account for the correlation effects, we simply divide by 2 the values of the band edges extracted by DFT, which corresponds to the mentioned increase of a factor 2 for the effective mass m_α and for the density of states N_α^0. The estimated band parameters in the presence of correlation are summarized in Table I.

In the presence of a retarded boson-mediated interaction, the Green's function $G_\alpha(z)$ for a generic band α can be written as

$$G_\alpha(\mathbf{k},\omega) = \frac{1}{\omega - \epsilon_{\mathbf{k},\alpha} - \chi_\alpha(\omega) + \mu + i\Gamma_\alpha(\omega)}, \tag{3}$$

TABLE I. Microscopic band parameters used in this work. Following the approach of Ref. 15, we use DFT band parameters renormalized by a factor 2 to account for the correlation effects.

Band index	m_α/m_e	$E_{\max,\alpha}$ (eV)	$E_{\min,\alpha}$ (eV)	N_α^0 (eV^{-1})
1	1.16	0.102	−2.516	0.382
2	2.28	0.102	−1.231	0.750
3,4	1.58	1.776	−0.147	0.520

where we introduced the short-hand notations

$$\chi_\alpha(\omega) = \text{Re}\Sigma_\alpha(\omega), \quad \Gamma_\alpha(\omega) = -\text{Im}\Sigma_\alpha(\omega).$$

The self-energy $\Sigma_\alpha(\omega)$ in the Matsubara space can be computed as

$$\Sigma_\alpha(i\omega_n) = -T\sum_{m,\beta} V_{\alpha,\beta} D(\omega_n - \omega_m) G_\beta(i\omega_m), \tag{4}$$

where $G_\beta(i\omega_m) = \int (d^2\mathbf{k}/4\pi^2) G_\beta(\mathbf{k}, i\omega_m)$ is the local one-particle Green's function, $D(\omega_l) = \int d\Omega 2\Omega B(\Omega)/(\Omega^2 + \omega_l^2)$ is the propagator of the bosonic mode, and $B(\Omega)$ is the density of states of the bosonic excitations. Here we assumed for simplicity that the interaction does not depend on the momentum, so that also the self-energy is momentum-independent. Finally, the self-energy $\Sigma_\alpha(\omega)$ and the Green's function $G_\alpha(\mathbf{k},\omega)$ on the real-frequency axis can be obtained employing the standard Marsiglio-Schossmann-Carbotte analytical continuation,[20] and the number of charge carriers per band can be obtained as

$$n_\alpha = N_s \int d\omega [1 - f(\omega)] N_\alpha(\omega), \quad \alpha = 1,2 \tag{5}$$

for the hole bands and

$$n_\alpha = N_s \int d\omega f(\omega) N_\alpha(\omega), \quad \alpha = 3,4 \tag{6}$$

for the electron bands, where $f(x) = 1/[\exp(x/T) + 1]$ is the Fermi function, $N_\alpha(\omega)$ is the interacting density of states (DOS), $N_\alpha(\omega) = N_\alpha^0 \int d\epsilon A(\epsilon,\omega)$, and where $A_\alpha(\epsilon_\mathbf{k},\omega) = -(1/\pi)\text{Im}G_\alpha(\mathbf{k},\omega + i0^+)$ is the one-particle spectral function.

To account for a spin-mediated interaction mechanism, we use here the Lorentzian spectrum[21]

$$B(\Omega) = \frac{1}{\pi} \frac{\Omega\omega_0}{\omega_0^2 + \Omega^2} \tag{7}$$

with a characteristic energy scale $\omega_0 = 20$ meV. From the above relations, we can introduce the matrix of the dimensionless coupling $\lambda_{\alpha,\beta} = V_{\alpha,\beta} N_\beta D(0)$, which is related to the low-energy mass renormalization due to the retarded interaction as $m_\alpha^* = (1 + \lambda_\alpha) m_a$, where $\lambda_a = \sum_\beta \lambda_{\alpha,\beta}$. Following Ref. 15, we take $V_{\alpha\beta} = V$ for the (α,β) values shown in Fig. 2, and $V_{\alpha\beta} = 0$ otherwise. This choice is appropriate for LaFePO, while for 122 pnictides the anisotropy of $V_{\alpha\beta}$ must be taken into account.[18] Nonetheless, all the results we will discuss below depend only quantitatively on the exact form of the spectrum and of the $V_{\alpha\beta}$ matrix, and will be qualitatively the same also for other choices of the boson mediator and of the interactions, provided that interband terms $V_{\alpha\beta}$, $\alpha \neq \beta$ dominate over the intraband ones.

As we discussed in Ref. 15, the strong particle-hole asymmetry of each band in pnictides forces us to calculate the Eliashberg self-energy by taking into account the finite bandwidth. In contrast to the usual infinite-band Eliashberg approximation, this leads to a finite value of $\chi_\alpha(\omega = 0)$, and to a corresponding change of size of the Fermi surface that depends on the interband versus intraband character of the interaction. In the case of dominant interband scattering, in particular, these finite-bandwidth self-energy effects result in a *shrinking* of the Fermi surface, whose new Fermi vectors can be obtained from the poles of the Green's function (3) as

$$k_{F,\alpha}^2 = \frac{2m_\alpha[E_{\max,\alpha} + \chi_\alpha(0)]}{\hbar^2} \tag{8}$$

for hole bands ($\alpha = 1,2$), while for electron bands ($\alpha = 3,4$) we have

$$k_{F,\alpha}^2 = \frac{2m_\alpha[|E_{\min,\alpha}| - \chi_\alpha(0)]}{\hbar^2}. \tag{9}$$

Note that, as shown in Ref. 15, for interband interactions $\chi_\alpha(0)$ is *negative* for the hole bands while it is *positive* for the electronic one, so that $k_{F,\alpha}$ is reduced in both cases. From the Fermi area we can define a *coherent* charge-carrier concentration per band:

$$\tilde{n}_\alpha = \frac{a^2 k_{F,\alpha}^2}{2\pi}, \tag{10}$$

where we have taken into account the spin degeneracy $N_s = 2$. In the case of a rigid band shift, as hypothesized in Ref. 16, $\tilde{n}_\alpha$ is also equivalent to the total charge-carrier concentration per band n_α. Things are, however, very different when the shrinking of the Fermi surface is induced by a retarded interaction mediated by a low-energy boson. Indeed, in this case although the reduction of the Fermi areas and hence of $\tilde{n}_\alpha$ is remarkable, the total charge-carrier concentration per band n_α is almost unaffected. Note that this result does not violate the Luttinger theorem, since for a multiband system there is no equivalence within each band between the charge concentration n_α and its corresponding Fermi area encoded in $\tilde{n}_\alpha$, as is instead the case in a single-band system. Indeed, the usual argument used to prove such an equivalence for the single-band case[22] shows that in the multiband case the Luttinger theorem only applies to the sum of the carrier density in all the bands. In Fig. 3, we plot the variation of both the total n_α and the coherent $\tilde{n}_\alpha$ carrier density for each band as a function of the corresponding band shift $\chi_\alpha(0)$, which is proportional to the coupling to the bosonic mode.[15] The corresponding shrinking of the Fermi area can be directly obtained by Eqs. (8) and (9). As one can see, a band shift $\chi_\alpha(0) \approx 25$ meV [that corresponds to the Fermi-surface shrinking observed experimentally in LaFePO (Refs. 1 and 15)] leads to a remarkable reduction of $\tilde{n}_\alpha$, up to almost 25%, whereas the reduction of n_α is much less pronounced, with the largest variations of n_α of the order of 5%.

To understand why the total charge-carrier concentration per band n_α is almost unaffected by the interaction in spite of the strong shrinking of the Fermi areas, let us examine the behavior of the interacting DOS $N(\omega)$. As an explicative

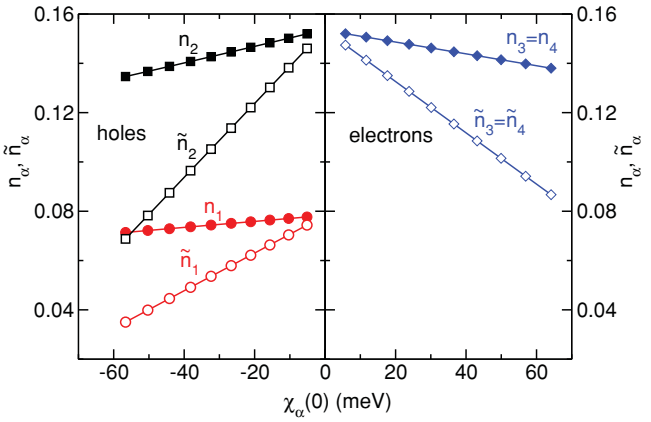

FIG. 3. (Color online) Variation of the hole and electron densities as a function of the energy shift at the Fermi surface. Here n_α is the total number of carriers in each band, while $\tilde{n}_\alpha$ is the number of coherent carriers related to the Fermi area according Eq. (10).

example, we compare in Fig. 4 the DOS of the electron band 3 in three cases: (a) without interaction, (b) in the presence of a rigid-band shift equivalent to $\chi_3(0)$, and (c) in the presence of the coupling to spin fluctuations. Here we used a relatively large value of the coupling [$V = 0.92$ eV, leading to $\chi_3(0) \approx 60$ meV] to make more visible in the figure the effects of the interaction. In each panel, the shaded area corresponds to the integral of the DOS up to Fermi level (i.e., $\omega = 0$ in our

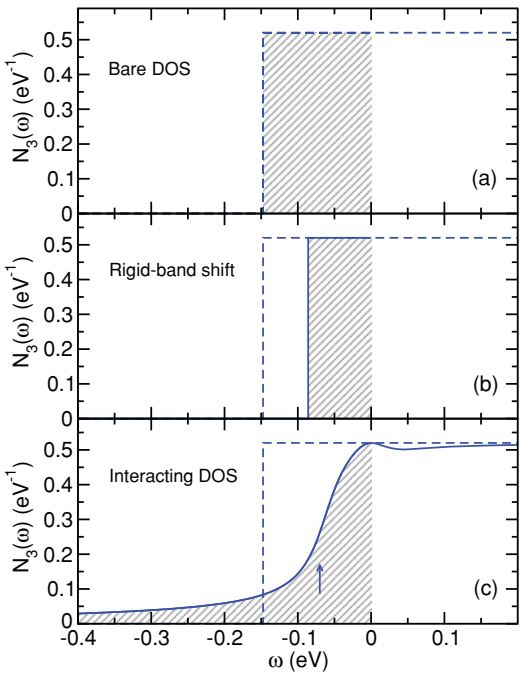

FIG. 4. (Color online) DOS of the electron band 3 in three representative cases: (a) bare DOS; (b) rigid-band shift; and (c) interacting case, computed using $V = 0.92$ eV. The shaded areas correspond to the particle number at $T = 0$ in the three cases. The arrow in panel (c) marks the new band edge due to the energy shift induced by $\chi_3(0)$. Note, however, that the DOS extends also below this limit due to the finite value $\Gamma_3(\omega)$ of the imaginary part of the self-energy.

notation), which gives the carrier density at $T = 0$ according to Eq. (6). In the case of a rigid-band shift, the number of carriers decreases following the Fermi-surface shrinking (10). However, as shown in Fig. 4(c), when the shrinking is due to a many-body interaction, the redistribution of spectral weight in the DOS is remarkably different. Here the presence of a finite $\chi_3(\omega)$ is reflected, in analogy with the rigid-band case, in a shift of the band bottom with respect to the noninteracting case, visible at the energy level where the quasiparticle DOS has a rapid drop [blue arrow in Fig. 4(c)]. However, this effect is balanced by a strong redistribution of spectral weight in an extended tail of the DOS for $\omega \lesssim E_{\min,3} = -0.15$ eV, which (almost) compensates for the band-edge shift and explains why n_3 is only slightly smaller than the bare value, as shown Fig. 3. Such a long tail in the DOS is due to the incoherent states induced by the imaginary part of the self-energy $\Gamma_3(\omega)$, and it is a characteristic signature of the interband nature of the interaction.

To better understand this issue, we plot in Fig. 5 both the DOS and the self-energy for bands 2 and 3 over a larger energy

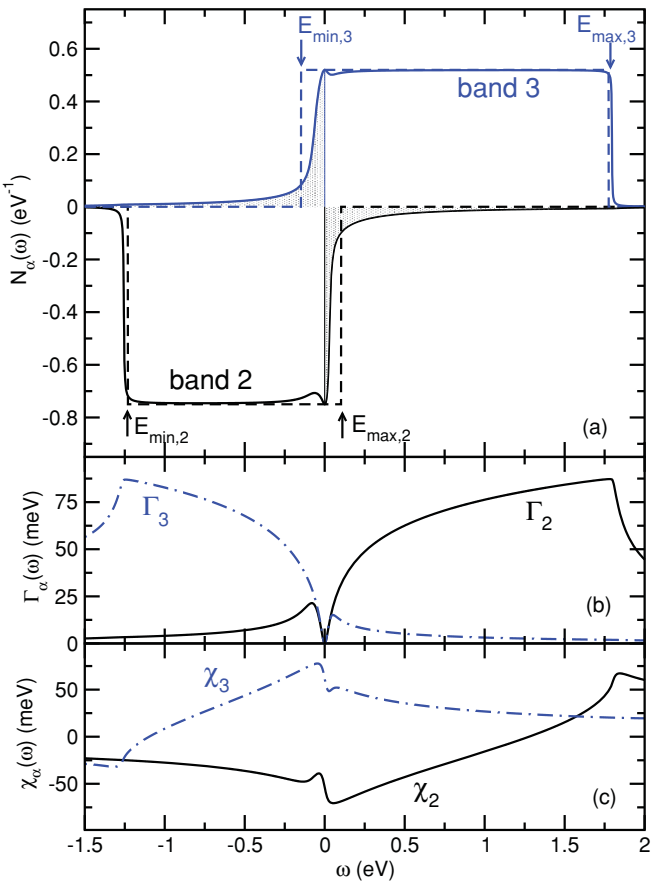

FIG. 5. (Color online) (a) DOS of the hole band 2 and of the electron band 3 (solid lines), displayed along with the bare DOS (dashed lines). To better resolve the two bands, we used a negative y axis for the DOS of the band 2. The shaded areas give the number of carriers n_α in each band at $T = 0$, according to Eqs. (5) and (6). (b) and (c) Energy dependence of the imaginary and of the real part of the self-energy for the same bands. Note that $\Gamma_2(\omega)$ is different from zero in an energy range corresponding to the DOS of the band 3, and vice versa.

scale, which allows us to show also that similar effects occur for both electron- and holelike bands. In panel Fig. 5(b), we compare the corresponding imaginary parts of the self-energy $\Gamma_\alpha(\omega)$. It is important to notice here that in the holelike band, $\Gamma_2(\omega)$ has a finite support that coincides approximately with the DOS of the electronic band $N_3(\omega)$. The same occurs for $\Gamma_3(\omega)$, which is controlled by the support of $N_2(\omega)$. This is a direct consequence of the interband character of the interaction, where the energy support of $\Gamma_\alpha(\omega)$ is determined by the DOS of the band β to which the band α is coupled. This situation has drastic effects on the resulting DOS. Indeed, as shown in Fig. 5(a), the incoherent states induced by $\Gamma_\alpha(\omega)$ are thus created mainly *outside* the energy range of the band α, that is, *below* the band bottom for the electron dispersions and *above* the band top for the hole ones, and they are responsible for the long tails in the corresponding DOS. It is worth stressing here that such tails are *not* due to a strong-coupling effect, but simply to a predominant interband nature of the interaction.

III. OPTICAL CONDUCTIVITY AND SPECTRAL WEIGHT

In the previous section, we have seen how the Fermi-surface shrinking generated by a retarded interaction is not directly reflected in a substantial reduction of the charge-carrier density n_α for the corresponding band, although the total number of coherent states $\tilde{n}_\alpha$ is strongly affected by that shrinking. As we shall see in the present section, such different behavior can be properly detected in the analysis of the optical properties. In particular, we show that the optical sum rule, which is directly related to total number of carrier n_α in each band, is almost unaffected by the Fermi-surface shrinking, whereas the dc conductivity and the spectral weight in the coherent Drude peak scale with $\tilde{n}_\alpha$, so that they are strongly reduced by the Fermi-surface shrinking, with a transfer of spectral weight to the intraband incoherent processes.

To address this issue, we compute explicitly the optical conductivity in the presence of the retarded interband interaction. Since for a **k**-independent self-energy the vertex corrections vanish, $\sigma(\omega)$ can be computed in the simple-bubble approximation. We can write thus $\sigma(\omega) = \sum_\alpha \sigma_\alpha(\omega)$, where

$$\sigma_\alpha(\omega) = -\frac{2\pi e^2}{\hbar}\int_{-\infty}^{\infty} dz \frac{f(z-\mu+\omega)-f(z-\mu)}{\omega} \times \int \frac{d^2\mathbf{k}}{(2\pi)^2} v_{\mathbf{k},\alpha}^2 A_\alpha(\varepsilon_{\mathbf{k},\alpha}, z+\omega) A_\alpha(\varepsilon_{\mathbf{k},\alpha}, z), \quad (11)$$

where $v_{\mathbf{k},\alpha} = (1/\hbar)\partial\varepsilon_{\mathbf{k},\alpha}/\partial k_x$ is the quasiparticle velocity, and the spectral function can be written explicitly as

$$A_\alpha(\varepsilon,\omega) = \frac{1}{\pi}\frac{\Gamma_\alpha^{\rm qp}(\omega)}{[\omega-\varepsilon-\chi_\alpha(\omega)]^2 + \left[\Gamma_\alpha^{\rm qp}(\omega)\right]^2}. \quad (12)$$

Here we considered also a finite contribution of disorder to the total quasiparticle scattering rate, $\Gamma_\alpha^{\rm qp}(\omega) \equiv \Gamma_\alpha(\omega) + \Gamma_0$. Since as $T \to 0$ $\Gamma_\alpha(0) \to 0$, we choose $\Gamma_0 = 10$ meV by estimating the approximate width of the low-energy optical spectra from Ref. 12 [see also Eqs. (20) and (21) below]. By converting the **k** integration in an energy integration and considering the parabolic holelike and electroniclike dispersions described in Eqs. (1) and (2), we obtain for the hole bands ($\alpha = 1,2$)

$$\sigma_\alpha(\omega) = -\frac{e^2}{\hbar}\int_{-\infty}^{\infty} dz \frac{f(z-\mu+\omega)-f(z-\mu)}{\omega} \times \int_{E_{\rm min}}^{E_{\rm max}} d\epsilon (E_{{\rm max},\alpha}-\varepsilon) A_\alpha(\varepsilon, z+\omega) A_\alpha(\varepsilon, z), \quad (13)$$

while for the electron bands ($\alpha = 3,4$)

$$\sigma_\alpha(\omega) = -\frac{e^2}{\hbar}\int_{-\infty}^{\infty} dz \frac{f(z-\mu+\omega)-f(z-\mu)}{\omega} \times \int_{E_{\rm min}}^{E_{\rm max}} d\epsilon (\varepsilon - E_{{\rm min},\alpha}) A_\alpha(\varepsilon, z+\omega) A_\alpha(\varepsilon, z). \quad (14)$$

The resulting optical conductivity $\sigma(\omega)$ at low temperature is shown in Fig. 6 for the same coupling value $V = 0.46$ eV used in Ref. 15 to reproduce the Fermi-surface shrinking measured by de Haas–van Alphen experiments in LaFePO. Also shown in the same plot is the integrated optical spectral weight $W(\omega) = \int_0^\omega d\omega' \sigma(\omega')$ as a function of the cutoff frequency. When the integration frequency goes to infinity, the total spectral weight is given by the optical sum rule, which for a parabolic-band approximation such as the one we are using here simply reduces to[10,11]

$$W = \int_0^\infty d\omega \sigma(\omega) = \frac{\pi e^2}{2}\sum_\alpha \frac{n_\alpha}{m_\alpha}. \quad (15)$$

This asymptotic value is marked in Fig. 6 by a solid arrow, along with the sum-rule value W_0 in the absence of the coupling to spin fluctuations. As we can see, the discrepancy between

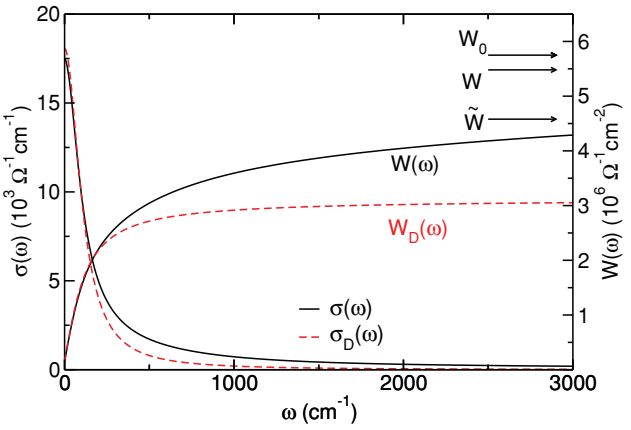

FIG. 6. (Color online) Left axis: Frequency dependence of the optical conductivity at $T = 5$ K as obtained from (13) and (14) (solid line), and low-energy Drude-like peak as obtained from Eq. (21) (dashed line). The small discrepancy for the dc values stems from the use of the approximate formulas (19) and (18) in the Drude term. To permit a simpler comparison with the experiments, we divided the two-dimensional results by the interlayer distance $d = 8.5$ Å. Right axis: integrated spectral weight $W(\omega)$, compared to the integral of the Drude part only, $W_D(\omega)$. The arrows mark the bare value W_0, the asymptotic value W (15) in the interacting case, and the value $\tilde{W}$ corresponding to the reduced Fermi surfaces.

W and W_0 turns out to be of order of 5%, pointing out that the effect of the Fermi-surface shrinking induced by the many-body interaction is quite small in the total sum rule. However, by direct inspection of Fig. 6, one can also see that even at frequencies $\omega \sim 3000$ cm^{-1}, corresponding to about $20\omega_0$, the collected spectral weight $W(\omega)$ still differs by about 20% from its asymptotic limit (15), and it is near instead to the spectral weight corresponding to a rigid-band shift, that is, $\tilde{W} = \pi e^2 \sum_\alpha \tilde{n}_\alpha / 2m_\alpha$. Such a lack of saturation of $W(\omega)$ over frequency scales much larger than the typical boson energy ω_0 is unusual for single-band systems,[23,24] and indicates that for the multiband case discussed here a large spectral contribution is allocated at relatively high energies.

To enlighten this issue and its relation to the Fermi-surface shrinking, let us first evaluate the dc conductivity in the zero-temperature limit, where we can write in Eqs. (13) and (14) $\lim_{\omega\to 0}[f(z-\mu+\omega)-f(z-\mu)]/\omega \approx -\delta(z-\mu)$. By performing the remaining integration over ε analytically, we thus get

$$\sigma_\alpha^{\rm dc} = \frac{e^2}{2\pi^2\hbar}\left\{1+\frac{|E_{\min,\alpha}|-\chi_\alpha(0)}{\Gamma_\alpha^{\rm qp}(0)}\left[\arctan\frac{E_{\max,\alpha}+\chi_\alpha(0)}{\Gamma_\alpha^{\rm qp}(0)} + \arctan\frac{|E_{\min,\alpha}|-\chi_\alpha(0)}{\Gamma_\alpha^{\rm qp}(0)}\right]\right\} \tag{16}$$

for the electrons and

$$\sigma_\alpha^{\rm dc} = \frac{e^2}{2\pi^2\hbar}\left\{1+\frac{E_{\max,\alpha}+\chi_\alpha(0)}{\Gamma_\alpha^{\rm qp}(0)}\left[\arctan\frac{|E_{\min,\alpha}|-\chi_\alpha(0)}{\Gamma_\alpha^{\rm qp}(0)} + \arctan\frac{E_{\max,\alpha}+\chi_\alpha(0)}{\Gamma_\alpha^{\rm qp}(0)}\right]\right\} \tag{17}$$

for the holes. For $T \to 0$ the only source of damping is due to disorder, so that $\Gamma^{\rm qp}(0)$ reduces to impurity scattering Γ_0. Since Γ_0 is usually much smaller than the distance of the band edge from the Fermi level [including also the shift $\chi(0)$], the above expressions simplify considerably. Indeed, using the expressions (8), (9), and (10), we obtain for the hole bands ($\alpha = 1,2$)

$$\sigma_{\rm dc}^\alpha = \frac{e^2}{2\pi\hbar\Gamma^{\rm qp}(0)}[E_{\max,\alpha}+\chi_\alpha(0)] = \frac{\tilde{n}_\alpha e^2\tau_{{\rm tr},\alpha}}{m_\alpha^*}, \tag{18}$$

and for the electron bands ($\alpha = 3,4$)

$$\sigma_{\rm dc}^\alpha = \frac{e^2}{2\pi\hbar\Gamma^{\rm qp}(0)}[|E_{\min,\alpha}|-\chi_\alpha(0)] = \frac{\tilde{n}_\alpha e^2\tau_{{\rm tr},\alpha}}{m_\alpha^*}, \tag{19}$$

where we introduced the effective mass $m_\alpha^* = (1+\lambda_\alpha)m_\alpha$ and the transport scattering time

$$\tau_{{\rm tr},\alpha}^{-1} = \frac{2\Gamma_\alpha^{\rm qp}(0)}{\hbar(1+\lambda_\alpha)}. \tag{20}$$

As is evident from Eqs. (18) and (19), even though the total carrier numbers n_α are almost unaffected by the shrinking of the Fermi areas (see Fig. 3), the dc conductivity is instead controlled by the coherent carrier density $\tilde{n}_\alpha$. More generally, one can generalize this result to finite frequency to get an approximate expression of the coherent Drude peak $\sigma^D(\omega)$ in the presence of the many-body interaction as

$$\sigma_\alpha^D(\omega) = \frac{\tilde{n}_\alpha e^2\tau_{{\rm tr},\alpha}}{m_\alpha^*}\frac{1}{1+(\omega\tau_{{\rm tr},\alpha})^2}. \tag{21}$$

The coherent Drude peak described in Eq. (21) is also shown in Fig. 6, along with its integrated spectral weight W_D on the right-side scale. The comparison with $W(\omega)$ shows that $W_D(\omega)$ saturates quite rapidly to its asymptotic value $\pi e^2\tilde{n}/2m^*$, while $W(\omega)$ steadily increases in this range of energies, showing that all the remaining spectral weight needed to recover the value (15) must originate from incoherent processes at higher frequencies. Note that this result has to be contrasted with the standard infinite-band case, where the real part of the self-energy vanishes and the spectral-weight distribution is only due to the mass renormalization, so that the coherent Drude part $W_D \propto n_\alpha/m_\alpha^*$ [see Fig. 1(a)].[11] On the contrary, here the many-body interaction gives rise to an additional Fermi-surface shrinking, which is reflected in a further reduction of the coherent spectral weight $\tilde{W} \propto \tilde{n}_\alpha/m_\alpha^*$ [see Fig. 1(c)].

IV. TEMPERATURE DEPENDENCE

In the previous section, we have seen that the many-body interband interaction plays a nontrivial role on the spectral properties of systems with strongly particle-hole asymmetric bands, and in particular in pnictides. This is pointed out, for instance, in the coherent contribution to the optical conductivity described in Eq. (21). In infinite bandwidth systems, assuming the bosonic spectrum $B(\Omega)$ to be weakly temperature-dependent, the main temperature dependence of the optical conductivity in Eq. (21) is through the parameter $\tau_{{\rm tr},\alpha}(T)$ [or equivalently $\Gamma_\alpha^{\rm qp}(T)$], whereas $\tilde{n} = n$ is temperature-independent. This scenario has to be contrasted with the case of a multiband system with strong particle-hole asymmetry, where the real part of the self-energy $\chi_\alpha(0)$, which gives rise to the Fermi-surface shrinking, is itself temperature-dependent and it is reflected in a coherent charge concentration $\tilde{n}_a$ which acquires a finite temperature dependence. Such a case will be analyzed in Sec. IV A, whereas in Sec. IV B we consider the additional effects due to a temperature-dependent bosonic spectrum, as suggested by a number of experiments in pnictides. In this case, the dimensionless electron-boson coupling λ_α and the low-energy mass renormalization $m_\alpha^*/m_\alpha = 1+\lambda_\alpha$ acquire their own temperature dependence, which can compete with the previously discussed effects. As we shall see, transport and optical properties can present quite different temperature behaviors in the two cases.

A. Temperature-independent bosonic spectrum

We consider first the case in which the bosonic spectrum is not itself temperature-dependent. In this case, the formalism is the same as we discussed so far, and we should only account for the temperature evolution of the self-energy. In Fig. 7, we show as an example the temperature dependence of the real and imaginary parts of the self-energy at zero frequency for band 2. As we can see, the absolute value of both quantities increases as the temperature increases, due to the thermal excitations of the bosonic mode. To get some analytical insight into these results, one can employ the first-order expansion for the self-energy, computed using the noninteracting Green's function in Eq. (4). The corresponding expression for $\chi_\alpha(0,T=0)$ has been derived in Ref. 15 in the case of an Einstein bosonic spectrum, $B(\Omega) = (\omega_{\rm E}/2)\delta(\Omega-\omega_{\rm E})$. By performing the same

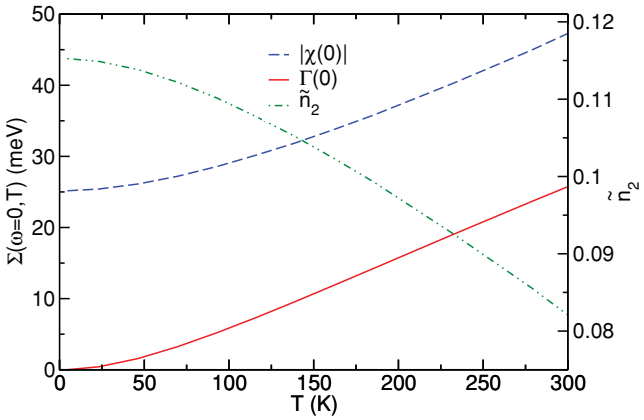

FIG. 7. (Color online) Left axis: temperature dependence of the real and imaginary part of the self-energy at zero frequency for band 2. Right axis: temperature dependence of the coherent carrier density $\tilde{n}_2$ obtained from the Fermi surface area according Eq. (10).

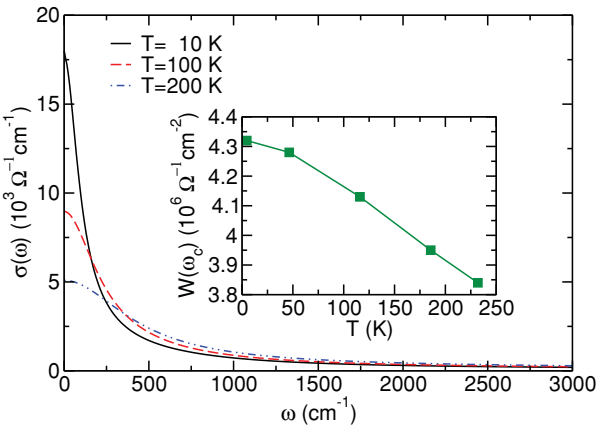

FIG. 8. (Color online) Optical conductivity for three representative temperatures $T = 10, 100$, and 200 K using a temperature-independent bosonic spectrum $B(\Omega)$ and an impurity scattering rate $\Gamma_0 = 10$ meV. Inset: temperature dependence of the integrated spectral weight $W(\omega_c)$ with $\omega_c = 3000$ cm^{-1}.

calculation at finite T, one can see that the most relevant temperature corrections are related to the thermal excitation of the boson:

$$\chi^E_\alpha(0,T) \approx -\frac{\omega_E}{2}\sum_\beta \lambda_{\alpha\beta} \ln\left|\frac{E_{\max,\beta}-\mu}{E_{\min,\beta}-\mu}\right| \times\left[1+\frac{2\omega_E}{E_{c,\beta}} b(\omega_E/T)\right], \quad (22)$$

where $E_{c,\beta} = \min(E_{\max,\beta}, E_{\min,\beta})$ is the nearest band edge, and $b(x) = 1/[\exp(x/T)-1]$ is the Bose function. In the case of a spin-fluctuation spectrum, the direct comparison with the results in Fig. 7 shows that a similar expression holds, provided the identification of the characteristic energy scale $\omega_E \approx 2\omega_0$. The imaginary part of the self-energy at zero frequency can also be computed exactly in the same approximation for temperatures $T \ll E_c$:

$$\Gamma^E_\alpha(0,T) \approx -\pi T \sum_\beta \lambda_{\alpha\beta}. \quad (23)$$

An analytical result can be derived for $\Gamma_\alpha(0,T)$ also for the spin-fluctuation spectrum, and we obtain

$$\Gamma_\alpha(0,T) \approx -2T \arctan\frac{T}{\omega_0}\sum_\beta \lambda_{\alpha\beta}, \quad (24)$$

which is in good agreement with the results of Fig. 7.

For what concerns the optical spectrum, the thermal excitation of the bosonic mode has then two consequences: (i) a further reduction of the Fermi surface areas, encoded in the decrease of $\tilde{n}_\alpha(T)$ with temperature, as shown in Fig. 7; and (ii) a progressive broadening of the optical-conductivity features, due to the increase of $\Gamma_\alpha(T)$. While the latter effect is customary also in the single-band infinite-bandwidth case, the former is particular to multiband systems with interband-dominating interactions, and leads to an unusual temperature dependence of the partial optical sum rule $W(\omega_c)$. Indeed, as we have seen in Sec. III, since the Fermi-surface shrinking gives rise to a transfer of spectral weight from the low-energy Drude peak $\propto \tilde{n}$ to the incoherent structure extending up to high energies, a finite temperature dependence of $\tilde{n}$ reflects directly in a sizable temperature-dependent depletion of $W(\omega_c)$ when a finite cutoff ω_c is employed.

In Fig. 8, we show the evolution of the optical conductivity for three different temperatures, using again the multiband scattering matrix $\lambda_{\alpha\beta}$ and the bosonic spectrum estimated in Ref. 15 to reproduce the Fermi-surface shrinking of LaFePO at $T \approx 10$ K. Here we assume the all these parameters are temperature-independent and we also use a constant impurity scattering rate $\Gamma_0 = 10$ meV. The corresponding variation of the spectral weight $W(\omega_c)$ as a function of the temperature is reported in the inset, showing an overall reduction of about 10%. Note that such a variation is an order of magnitude larger than the one expected in a single-band system for the same coupling value, even when the presence of a finite bandwidth[24,25] and a finite cutoff[26,27] are taken into account. Quite remarkably, this temperature variation is as large as the one observed in cuprate superconductors, where it has been interpreted as a consequence of strong correlations.[10,11,23] In our case, however, this effect comes primarily from the temperature dependence of the coherent carriers number, which is relatively large even when the coupling to the bosonic mode is not particularly strong.

B. Temperature-dependent bosonic spectrum

As we have seen in Sec. III, the low-energy part of the optical spectrum resembles a renormalized Drude model, with an inverse scattering time τ_{tr}^{-1} proportional to the imaginary part of the self-energy. As a consequence, if the boson spectrum is constant in temperature, the broadening of the optical conductivity as the temperature increases is directly proportional to the increase of $\Gamma_\alpha(0)$, as shown, for instance, in the case of Fig. 8. With this choice, however, we get an optical width of the Drude-like low-frequency part at room temperature of about 600 cm^{-1}, much larger than the scattering rate $\tau_{tr}^{-1} \simeq 320$ cm^{-1} that can be fitted from the available experimental data at $T = 300$ K.[12] This

observation suggests thus that the increase of $\Gamma_\alpha(0)$ with temperature is smaller than predicted by Eq. (23). To account for this discrepancy, we investigate here the possibility that the bosonic spectrum is itself temperature-dependent, as has been suggested also by a recent analysis of optical spectra in 122 compounds.[28] In particular, in Ref. 28 it has been shown that the bosonic spectrum extracted from optics hardens as T increases, while its total spectral weight, encoded in the dimensionless couplings $\lambda_{\alpha\beta}$, decreases. This trend is also consistent with direct measurements of the spin-fluctuations spectrum by means of neutron scattering in 122 compounds.[29] Following Ref. 29, we model such behavior by assuming a temperature-dependent bosonic spectrum of the form

$$B(\Omega) = \frac{h(T)}{\pi} \frac{\bar{\omega}_0 \omega}{\omega^2 + \bar{\omega}_0^2}, \tag{25}$$

where

$$h(T) = \frac{T_\theta}{T + T_\theta} \tag{26}$$

and

$$\bar{\omega}_0(T) = \frac{\omega_0}{h(T)}. \tag{27}$$

We chose the value of $T_\theta = 150$ K to reproduce the experimental value of the Drude peak in the optical data of LaFePO at $T = 300$ K.[12] The evolution of the spectrum $B(\Omega)$ for three representative temperatures $T = 0, 100$, and 300 K and the corresponding temperature dependence of the coupling constant are shown in Figs. 9(a) and 9(b), respectively. Focusing for simplicity once again on band 2, we plot in panel (c) the resulting real and imaginary parts of the self-energy, $\chi_2(0)$ and $\Gamma_2(0)$. As one can see, for this choice of parameters the reduction of $\lambda_2(T)$ is strong enough to result in a *decrease* of $|\chi_2(0)|$ with the temperature and in a smaller increase of $\Gamma_2(0)$. As a consequence, also the temperature evolution of the optical conductivity, shown in

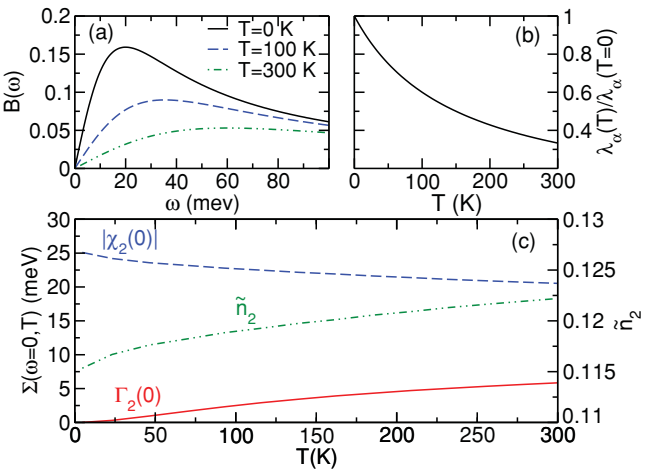

FIG. 9. (Color online) (a) Temperature evolution of the bosonic spectrum according to Eqs. (25)—(27). (b) Temperature evolution of the dimensionless coupling constant in each band. (c) Corresponding temperature dependence of $\chi_2(0)$ and $\Gamma_2(0)$ (left axis) and of $\tilde{n}_\alpha$ (right axis) in band 2 using the temperature-dependent bosonic spectrum $B(\Omega)$ of panel (a).

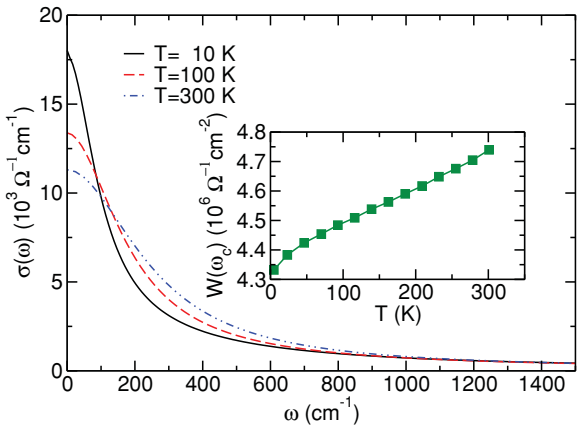

FIG. 10. (Color online) Optical conductivity for three representative temperatures using the temperature-dependent bosonic spectrum $B(\Omega)$ shown in Fig. 9(a). Here we used a constant impurity scattering rate $\Gamma_0 = 10$ meV. Inset: temperature dependence of the integrated spectral weight $W(\omega_c)$ with $\omega_c = 3000$ cm^{-1}.

Fig. 10, is markedly different than before. In particular, the reduction of $|\chi_\alpha(0)|$ with the temperature is reflected now in an *increase* of $\tilde{n}_\alpha(T)$ [see Fig. 9(c)]. The spectral weight moves thus progressively toward the low-energy coherent part of the spectrum, leading also to an effective increase of the spectral weight $W(\omega_c)$ integrated in a fixed frequency window, in sharp contrast to what is expected in ordinary single-band (interacting and noninteracting) systems.[10,11,23]

V. COMPARISON WITH THE EXPERIMENTS

Even though a detailed comparison with the experimental optical spectra is beyond the scope of the present paper, we would like to comment on the possible consequences of our findings for the physics of pnictides. A first issue concerns the role of the cutoff in the estimate of both the absolute value of the spectral weight and its temperature dependence. From the experimental point of view, a finite cutoff ω_c is always employed in the estimate of the sum rule to avoid inclusion of interband transitions, so that $W_{\rm exp} \sim W(\omega_c)$. In pnictides, the choice of ω_c is dictated by the observed threshold to interband transitions, which usually occurs around $\omega_c =$ 2000–3000 cm^{-1}. This is indeed the case in Ref. 12, where the experimental estimate $W_{\rm exp}$ for LaFePO includes only processes up to a cutoff frequency of $\omega_c = 3000$ cm^{-1}. As we have shown in Fig. 6, the calculated spectral weight collected up to this same cutoff is about 20% of its asymptotic value W, which is instead almost unchanged (within ~5%) from the bare value W_0. While comparing with the experiments, we must recall that our starting model has renormalized DFT bands, so that $W_0 = 0.5 W_{\rm DFT}$. As a consequence, after inclusion of the low-energy spin fluctuations, we estimate overall $W(\omega_c) \simeq 0.4 W_{\rm DFT}$, that is, the main source of spectral-weight reduction still comes from correlation effects. We observe, however, that for the range of parameters used here, $W(\omega_c)$ is very near to the spectral weight $\tilde{W}$ that one would obtain from a

rigid-band shift. The reason is that, as we have seen in Sec. II, the incoherent part of each spectral function extends up to energy scales of the order of the bandwidth of the coupled band, that is, over energy scales much larger than the typical boson energy ω_0. As a consequence, even though there is no theoretical sum rule relating $W(\omega_c)$ to $\tilde{W}$, on the energy scales considered in the experiments this could be a good approximation for it. Note, however, that the situation could be slightly different in the 122 compounds, where the most populated band is also the less coupled to spin fluctuations,[18] making it difficult to predict *a priori* in a precise quantitative way the relevance of the shrinking on the absolute value of the optical sum rule with respect to DFT.

A more direct effect of the Fermi-surface shrinking on the optical data is instead the temperature dependence of the sum rule. Indeed, as we discussed in the previous section, the temperature dependence of $W(\omega_c)$ is strongly affected by the temperature evolution of the coherent charge density $\tilde{n}_\alpha$, which in turn is an indirect probe of the temperature evolution of the spin-fluctuation spectrum. Quite interestingly, recent optical measurements in both carrier-doped[30,31] and isovalent-substituted[32] 122 compounds show that $W_{\rm exp}$ increases with increasing temperature, in contrast to any ordinary behavior in a single-band system.[10,11,23] Within our scenario, this suggests that the coupling to the spin fluctuations is actually temperature-dependent, leading to an increase of $\tilde{n}_\alpha$ as the temperature increases, see Fig. 9(c), and to a progressive population of the low-energy optical spectrum, see Fig. 10. It is worth noting that our approach completely neglects the role of optical ($\mathbf{q} = \mathbf{0}$) interband transitions, which are presumably less relevant than the single-band transitions in the range of frequencies considered here. However, a detailed analysis of the role of these interband transitions and of their possible relevance in the experiments is at the moment an open question that deserves further theoretical investigation.

A third outcome of our results is related to the possible observation of these anomalous temperature behaviors in the dc transport properties. Indeed, from the approximate expressions (18) and (19) for the dc conductivity, it is clear that as the temperature increases, both $\tilde{n}_\alpha(T)$ and $\Gamma_a(T)$ contribute to the temperature dependence of the dc conductivity. In other words, for a multiband system with dominant interband interactions, one cannot simply attribute the T dependence of the resistivity to scattering processes, since also the density of coherent carriers can have a nontrivial temperature dependence. This observation could shed new light also on the comparative analysis of dc and Hall conductivities carried out in Refs. 33 and 34, where part of the anomalous behavior reported there could be accounted for by relaxing the assumption of a constant density of carriers with the temperature.

VI. CONCLUSIONS

In this paper, we analyzed systematically the behavior of the optical-conductivity sum rule in a multiband system with dominant interband interactions, as is the case in pnictide superconductors. Due to the strong particle-hole asymmetry of these systems, the coupling to a collective mode leads to a many-body induced band shift and to a corresponding shrinking of the Fermi surface areas. In this context, we have shown, however, that the number of particles in each band does not scale with the Fermi areas, but it is almost unchanged. Such behavior has been explained in terms of a transfer of the spectral weight from the coherent states related to the reduced Fermi areas to the unoccupied part of the noninteracting bands. As we have discussed in the present paper, the effects of such redistribution of spectral weight on the optical spectrum are quite different from what is expected in single-band systems. In particular, we have shown that only a fraction $\sim\tilde{n}/m^*$ of the total weight $\sim n/m$ is collected in the coherent low-energy part of the spectrum, while the rest is recovered as higher-energy incoherent processes. As a consequence, the unavoidable use of a finite cutoff ω_c in the experimental determination of the optical sum rule is expected to have a much stronger effect than in the single-band case. There are two main consequences. (i) $W_{\rm exp}$ usually underestimates the theoretical sum-rule value W in a percentage that cannot be established *a priori*, since it depends on the parameter values. In the case of LaFePO discussed here, $W_{\rm exp}$ turns out to be about 20% smaller than W. As a consequence, if one assumes that W is already strongly reduced ($\sim$50%) by correlations,[8,9] the many-body effect due to spin fluctuations is a small fraction ($\sim$10%) of the DFT value $W_{\rm DFT}$. (ii) The temperature evolution of the optical sum rule turns out to be an indirect measurement of the temperature evolution of the Fermi-surface areas. For instance, a temperature dependence of the spin-fluctuation spectrum could suggest that the ω-integrated spectral weight $W(\omega_c)$ could *increase* with temperature, in sharp contrast to the case of interacting single-band systems, as, for example, cuprate superconductors. All these findings pose strong constraints on the analysis of optical data in Fe-based materials, showing once more that the peculiar semimetal and multiband character of these systems forces us to revise standard paradigms appropriate for single-band correlated materials.

ACKNOWLEDGMENTS

We thank C. Castellani, L. Boeri, and L. Ortenzi for useful discussions. This work has been supported in part by the Italian MIUR under the project PRIN 2007FW3MJX and PRIN 2008XWLWF9.

[1] A. I. Coldea, J. D. Fletcher, A. Carrington, J. G. Analytis, A. F. Bangura, J.-H. Chu, A. S. Erickson, I. R. Fisher, N. E. Hussey, and R. D. McDonald, Phys. Rev. Lett. **101**, 216402 (2008).

[2] J. G. Analytis, C. M. J. Andrew, A. I. Coldea, A. McCollam, J.-H. Chu, R. D. McDonald, I. R. Fisher, and A. Carrington, Phys. Rev. Lett. **103**, 076401 (2009).

[3] H. Shishido, A. F. Bangura, A. I. Coldea, S. Tonegawa, K. Hashimoto, S. Kasahara, P. M. C. Rourke, H. Ikeda, T. Terashima, R. Settai, Y. Onuki, D. Vignolles, C. Proust, B. Vignolle, A. McCollam, Y. Matsuda, T. Shibauchi, and A. Carrington, Phys. Rev. Lett. **104**, 057008 (2010).

[4]D. H. Lu, Nature (London) **455**, 81 (2008); D. H. Lu, M. Yi, S.-K. Mo, J. G. Analytis, J.-H. Chu, A. S. Erickson, D. J. Singh, Z. Hussain, T. H. Geballe, I. R. Fisher, and Z.-X. Shen, Physica C **469**, 452 (2009).

[5]L. X. Yang, Y. Zhang, H. W. Ou, J. F. Zhao, D. W. Shen, B. Zhou, J. Wei, F. Chen, M. Xu, C. He, Y. Chen, Z. D. Wang, X. F. Wang, T. Wu, G. Wu, X. H. Chen, M. Arita, K. Shimada, M. Taniguchi, Z. Y. Lu, T. Xiang, and D. L. Feng, Phys. Rev. Lett. **102**, 107002 (2009).

[6]L. Wray, D. Qian, D. Hsieh, Y. Xia, L. Li, J. G. Checkelsky, A. Pasupathy, K. K. Gomes, C. V. Parker, A. V. Fedorov, G. F. Chen, J. L. Luo, A. Yazdani, N. P. Ong, N. L. Wang, and M. Z. Hasan, Phys. Rev. B **78**, 184508 (2008).

[7]M. Yi, D. H. Lu, J. G. Analytis, J.-H. Chu, S.-K. Mo, R.-H. He, X. J. Zhou, G. F. Chen, J. L. Luo, N. L. Wang, Z. Hussain, D. J. Singh, I. R. Fisher, and Z.-X. Shen, Phys. Rev. B **80**, 024515 (2009).

[8]M. Aichhorn, L. Pourovskii, V. Vildosola, M. Ferrero, O. Parcollet, T. Miyake, A. Georges, and S. Biermann, Phys. Rev. B **80**, 085101 (2009).

[9]S. L. Skornyakov, A. V. Efremov, N. A. Skorikov, M. A. Korotin, A. Yu. Izyumov, V. I. Anisimov, A. V. Kozhevnikov, and D. Vollhardt, Phys. Rev. B **80**, 092501 (2009).

[10]See, for example, L. Benfatto and S. Sharapov, Low Temp. Phys. **32**, 533 (2006), and references therein.

[11]D. N. Basov, R. D.Averitt, D. van der Marel, M. Dressel, and K. Haule, Rev. Mod. Phys. (to be published).

[12]M. M. Qazilbash, J. J. Hamlin, R. E. Baumbach, L. Zhang, D. J. Singh, M. B. Maple, and D. N. Basov, Nat. Phys. **5**, 647 (2009).

[13]K. Kuroki, S. Onari, R. Arita, H. Usui, Y. Tanaka, H. Kontani, and H. Aoki, Phys. Rev. Lett. **101**, 087004 (2008).

[14]A. V. Chubukov, D. Efremov, and I. Eremin, Phys. Rev. B **78**, 134512 (2008).

[15]L. Ortenzi, E. Cappelluti, L. Benfatto, and L. Pietronero, Phys. Rev. Lett. **103**, 046404 (2009).

[16]I. Mazin, e-print arXiv:0910.4117.

[17]M. M. Qazilbash, J. J. Hamlin, R. E. Baumbach, L. Zhang, D. J. Singh, M. B. Maple, and D. N. Basov, e-print arXiv:1001.0643.

[18]L. Benfatto, E. Cappelluti, and C. Castellani, Phys. Rev. B **80**, 214522 (2009).

[19]It is clear that this value does not represent the true band edge as given in DFT, but an effective one needed to guarantee the total number of states.

[20]F. Marsiglio, M. Schossmann, and J. P. Carbotte, Phys. Rev. B **37**, 4965 (1988).

[21]A. J. Millis, Phys. Rev. B **45**, 13047 (1992).

[22]J. M. Luttinger and J. C. Ward, Phys. Rev. **118**, 1417 (1960).

[23]J. P. Carbotte and E. Schachinger, J. Low Temp. Phys. **144**, 61 (2006).

[24]A. E. Karakozov and E. G. Maksimov, Solid State Commun. **139**, 80 (2006).

[25]L. Benfatto, J. P. Carbotte, and F. Marsiglio, Phys. Rev. B **74**, 155115 (2006).

[26]M. R. Norman, A. V. Chubukov, E. van Heumen, A. B. Kuzmenko, and D. van der Marel, Phys. Rev. B **76**, 220509(R) (2007).

[27]S. Maiti and A. V. Chubukov, Phys. Rev. B **81**, 245111 (2010).

[28]D. Wu, N. Barisic, M. Dressel, G. H. Cao, Z-A. Xu, J. Carbotte, and E. Schachinger, Phys. Rev. B **82**, 144519 (2010).

[29]D. S. Inosov, J. T. Park, P. Bourges, D. L. Sun, Y. Sidis, A. Schneidewind, K. Hradil, D. Haug, C. T. Lin, B. Keimer, and V. Hinkov, Nat. Phys. **6**, 178 (2010).

[30]A. Lucarelli, A. Dusza, F. Pfuner, P. Lerch, J. G. Analytis, J.-H. Chu, I. R. Fisher, and L. Degiorgi, New J. Phys. **12**, 073036 (2010).

[31]N. Barisic, D. Wu, M. Dressel, L. J. Li, G. H. Cao, and Z. A. Xu, Phys. Rev. B **82**, 054518 (2010).

[32]D. Wu, G. Chanda, H. S. Jeevan, P. Gegenwart, and M. Dressel, e-print arXiv:1011.1207, to appear in Phys. Rev. B.

[33]F. Rullier-Albenque, D. Colson, A. Forget, and H. Alloul, Phys. Rev. Lett. **103**, 057001 (2009).

[34]F. Rullier-Albenque, D. Colson, A. Forget, P. Thuéry, and S. Poissonnet, Phys. Rev. B **81**, 224503 (2010).